R. & M. No. 3452

MINISTRY OF AVIATION

AERONAUTICAL RESEARCH COUNCIL
REPORTS AND MEMORANDA

Studies of Slotted-Wall Interference using an Electrical Analogue

By K. R. Rushton, Ph.D.

Part I.—The Electrical Analogue to Steady and Oscillating Flow in Slotted-Wall Tunnels

Part II.—Particular Examples of Slotted-Wall Tunnel Interference in Steady Flow

LONDON: HER MAJESTY'S STATIONERY OFFICE
1967

PRICE 13*s.* 0*d.* NET

Studies of Slotted-Wall Interference using an Electrical Analogue

By K. R. Rushton, Ph.D.

COMMUNICATED BY PROFESSOR S. C. REDSHAW, DEPARTMENT OF CIVIL ENGINEERING, UNIVERSITY OF BIRMINGHAM

Reports and Memoranda No. 3452*
June, 1965

Part I.—The Electrical Analogue to Steady and Oscillating Flow in Slotted-Wall Tunnels

Summary,

Part I of this report describes a study of the lift interference effect in slotted-wall wind tunnels performed by a pure resistance electrical analogue. Both steady and oscillatory flow are considered. Special techniques devised to represent the singular behaviour of a point wing and at the edges of each slot are discussed in detail. Comparisons are made with an exact solution based on an equivalent homogeneous boundary condition for steady flow. For oscillatory flow experimental results are presented which show how the magnitude of the interference upwash changes with the frequency of the oscillation.

1. *Introduction,*

Many of the wind tunnels used for both subsonic and transonic investigations have partially open walls consisting either of longitudinal slots or circular perforations. The boundaries of the tunnel influence the flow around the model, and there are several distinct interference effects, such as blockage interference on the stream velocity, lift interference on the model incidence and shock wave reflections from the walls. In oscillatory compressible flow tunnel wall resonance may occur. A recent review of unsteady interference effects in slotted-wall tunnels by Wight[1] describes the exceedingly large changes in pitching damping which may result from sealing off the slots. The present investigation concerns steady flow when linearised boundary conditions are applied at the slots. The study is carried out by means of a pure resistance electrical analogue with the object of obtaining detailed information about the lift interference in the wake of the wing and the flow near to the slots.

The resistance network automatically solves the two dimensional differential equation which is assumed to describe the potential function in the distant wake of an oscillating wing. In effect the resistance network is an automatic means of solving the finite difference equation, and in using a finite difference approach two particular difficulties arise. The first concerns the representation of the discontinuities in the velocity at the edge of the slots, and is overcome by the introduction of special singularity formulae at these points. The second problem arises from the necessity of obtaining accurate values of the interference potential,

*Part I replaces. A.R.C. 26680.
Part II replaces. A.R.C. 27140.

which are of a smaller order than the velocity potential. This is achieved by carrying out separate experiments, first in terms of the velocity potential and then in terms of the interference potential.

The reduction of the problem to two dimensions involves the assumption that the tunnel is cylindrical and of finite length, so that the velocity field becomes periodic in streamwise distance far downstream. For steady incompressible flow the velocity potential far downstream is known to equal twice the potential at the wing[2] and therefore the results for steady flow are directly relevant to the transverse plane containing the model, but for unsteady flow no such relationship exists and the results in the infinite wake can only be used as a rough indication of the amplitude, but not the phase, of the velocity field in the plane of the wing. Another assumption is the linearised condition at the slots, but any more accurate representation of the free boundary would involve a far more complicated network.

The resistance network is used to compare the interference upwash in steady flow for tunnels having different types of roof, including open and closed roofs, different slot configurations and an equivalent homogeneous condition. A further object of the report is to investigate whether failure of the linearised condition is a possible explanation of the large interference effects reviewed in Ref. 1.

2. *Mathematical Formulation,*

The problem of the interference upwash effect in slotted wind tunnels in linearised compressible flow leads on formulation to a second order partial differential equation in terms of the perturbation velocity potential. The boundary conditions for the tunnel walls and roof including the effect of the slots can be written in terms of the velocity potential and its normal slope. Many forms of wing could be adopted but for computational convenience a 'point' wing is selected. The perturbation velocity potential Φ_m for the point wing in an infinite field is known and this can be corrected to allow for the interference effects. If Φ is the actual perturbation velocity potential within the tunnel then the interference velocity potential, Φ_i can be determined from,

$$\Phi = \Phi_m + \Phi_i. \tag{1}$$

2.1. *Governing Differential Equation.*

For a field as shown in Fig. 1 with an undisturbed stream velocity U, the component velocities of the flow in the x, y and z directions are $U+u$, v and w.

These velocities can be expressed in terms of the perturbation velocity potential in linearised compressible flow, Φ, as

$$u = \partial\Phi/\partial x,\ v = \partial\Phi/\partial y \text{ and } w = \partial\Phi/\partial z, \tag{2}$$

and the governing equation for unsteady flow at Mach number M is

$$(1-M^2)\frac{\partial^2\Phi}{\partial x^2}+\frac{\partial^2\Phi}{\partial y^2}+\frac{\partial^2\Phi}{\partial z^2} = \frac{M^2}{U^2}\left(\frac{\partial^2\Phi}{\partial t^2}+2U\frac{\partial^2\Phi}{\partial x\partial t}\right). \tag{3}$$

If the tunnel geometry is independent of x and the wing is oscillating with angular frequency, ω, then it may be assumed that in the distant wake

$$\Phi = \text{Real part of } [\phi(y,z)e^{i\omega(t-x/U)}]. \tag{4}$$

Equations (3) and (4) lead to the differential equation for $\phi\ (y,z)$

$$\frac{\partial^2\phi}{\partial y^2}+\frac{\partial^2\phi}{\partial z^2} = (\omega/U)^2\phi, \tag{5}$$

which is seen to be independent of Mach number.

2.2. *Condition on the Tunnel Boundary.*

The tunnel is taken to have a rectangular cross section with solid side walls and ventilated roof and floor with four slots in each. The geometry of the quarter tunnel is explained in Fig. 2. On the boundaries of the tunnel two conditions hold.

(i) For a closed boundary the normal gradient of the velocity potential must vanish, hence on the walls,

$$\partial\phi/\partial y = 0 \text{ when } y = \pm\tfrac{1}{2}b,$$

and on the closed portion of the roof and floor

$$\partial\phi/\partial z = 0 \text{ when } z = \pm\tfrac{1}{2}h.$$

(ii) On the free boundary of the open portion of the tunnel, that is across the slots, there is a further condition for constant pressure, that

$$\left(U + \frac{\partial\Phi}{\partial x}\right)^2 + \left(\frac{\partial\Phi}{\partial y}\right)^2 + \left(\frac{\partial\Phi}{\partial z}\right)^2 = U^2. \tag{6}$$

The usual assumption in wall interference problems is that the free boundaries are not distorted by the presence of the wing, that the streamline condition is relaxed and that equation (6) can be linearised with respect to the perturbation velocity potential so that across the slots,

$$\Phi = \text{constant} = 0, \text{ i.e. } \phi = 0.$$

At the edge of the slot the boundary condition changes suddenly from (i) to (ii) with the result that a discontinuity in the slope of the function will occur. Also it should be noted that the boundary condition (ii) is very much idealised, and it would be desirable to simulate the free boundary condition more accurately.

Instead of separate conditions on the slots and slats of the tunnel, an equivalent homogeneous condition has been suggested[3]. In this method the overall effect of the slotted roof or floor is given by

$$\begin{gathered}\phi + K\,\partial\phi/\partial z = 0 \text{ for } z = \pm\tfrac{1}{2}h \\ \text{where } K = \frac{l}{\pi}\log_e \operatorname{cosec}\frac{\pi a}{2l};\end{gathered} \tag{7}$$

here l is the periodic slot spacing and a/l the open area ratio, Fig. 2.

2.3. *Flow Field of a Small Wing.*

It is now necessary to define the actual wing which is placed in the tunnel and then find its effect far downstream where $\phi\ (y,z)$ is to be determined. From the analytical solution for a very small wing in an infinite field of fluid, 'boundary' values for $\phi = \phi_m + \phi_i$ can be specified on $z = 0$.

Let the velocity potential of the perturbed flow.

$$\Phi = \text{Real part of } [\bar{\phi}(x,y,z)e^{i\omega t}] \tag{8}$$

where $\bar{\phi}$ is antisymmetric in z, (Reference 4). On the plane $z = 0$ downstream of the wing of span $2s$,

$$\left.\begin{aligned} \bar{\phi}(x,y,0+) &= -\bar{\phi}(x,y,0-) \text{ for } |y| \leqslant s, \\ \bar{\phi}(x,y,0) &= 0 \qquad\qquad \text{for } |y| > s. \end{aligned}\right\} \tag{9}$$

In the wake ($x>0$, $|y| \leqslant s$, $z = 0$)

$$U\,\partial\bar{\phi}/\partial x + i\omega\bar{\phi} = 0, \tag{10}$$

since there is no discontinuity in pressure there. For a wing of very small chord with uniform spanwise loading the lift is specified as

$$\begin{aligned} &\text{Real part of } [4s\rho U\bar{\phi}(0,y,0+)e^{i\omega t}] \\ &= \text{Real part of } [\tfrac{1}{2}\rho U^2 S C_L e^{i\omega t}]; \end{aligned} \tag{11}$$

with this condition at $x = 0$ equations (9) and (10) give

$$\bar{\phi}(x,y,0+) = \frac{USC_L}{8s} e^{-i\omega x/U} = -\bar{\phi}(x,y,0-) \text{ for } y \leqslant s. \tag{12}$$

In the limit as $x \to \infty$ equation (12) gives the boundary condition

$$\left.\begin{aligned} \phi(y,0+) &= \frac{USC_L}{8s} \text{for } |y| \leqslant s \\ \phi(y,0+) &= 0 \qquad \text{for } |y| > s \end{aligned}\right\} \tag{13}$$

to be satisfied by $\phi\,(y,z)$ of equation (4). In the limit as $s \to 0$ the solution of the governing differential equation (5) subject to (13) and the boundary conditions of an infinite field is

$$\phi(y,z) = \phi_m(y,z) = \frac{USC_L}{4\pi} \frac{\omega z}{Ur} K_1\left(\frac{\omega r}{U}\right), \tag{14}$$

where $r^2 = y^2 + z^2$ and $K_1\,(\omega r/U)$ is a Bessel function in the usual notation. Since $K_1\,(\omega r/U)$ satisfies the ordinary differential equation

$$K_1'' + \frac{1}{\omega r/U} K_1' = \left(1 + \frac{1}{(\omega r/U)^2}\right) K_1, \tag{15}$$

it can be verified that equation (14) is a particular solution of equation (5). Moreover, for small r equation (14) becomes

$$\phi(y,z) = \frac{USC_L}{4\pi} \frac{\omega z}{Ur} \left[\frac{U}{\omega r} + 0\left(\frac{\omega r}{U} \log \frac{\omega r}{U}\right)\right],$$

so that

$$\int_{-s}^{s} \phi(y,z)dy = \frac{USC_L}{4\pi}\left[2\tan^{-1}\frac{s}{z}+0\left(\frac{\omega z}{U}\right)\right]$$

$$= \frac{USC_L}{4} \text{ as } z\to 0, \tag{16}$$

which is consistent with equation (13).

The problem is to solve the two-dimensional differential equation (5) subject to the boundary conditions in Fig. 2 (Section 2.2). Since these are independent of Mach number, so are the solutions for ϕ and $\phi_i = \phi - \phi_m$.

2.4. *Determination of the Scaling Factor.*

For a wing of small span ϕ_m is given by equation (14). Let the electrical potential representing ϕ_m on the network be V_m where

$$V_m = \frac{4\pi F' h\phi_m}{USC_L} \tag{17}$$

in which F' is a scaling factor.

For steady flow the expression for ϕ_m is

$$\phi_m = \frac{USC_L}{4\pi}\frac{z}{r^2}$$

and hence the electrical potential becomes

$$V_m = hF'z/r^2. \tag{18}$$

For convenience the scale factor, F', is chosen to be $10\,000 \times 6/88$. Hence all measurements on the electrical network must be multiplied by a factor such that

$$\phi^m = \frac{USC^L}{4\pi h}\frac{88}{60\,000}V_m. \tag{19}$$

It should be noted that the same scaling factor is used both for steady and unsteady problems.

3. *The Electrical Analogue.*

The analogy between the finite difference form of partial differential equations and the electrical equations to resistance network has been used in the study of many field problems[5,6]. In this instance an analogous network to a second order partial differential equation is required and is devised in the following manner.

The equation

$$\frac{\partial^2\phi}{\partial y^2}+\frac{\partial^2\phi}{\partial z^2} = (\omega/U)^2\phi \tag{5}$$

must first be written in finite difference form,

$$\phi_1+\phi_2+\phi_3+\phi_4-4\phi_0 = (\omega/U)^2 d^2\phi_0 \tag{20}$$

where d is the mesh interval and the nodes are numbered as shown in Fig. 3a. Now for the electrical network of Fig. 3b the sum of currents entering the node 0 must be zero; hence

$$\frac{V_1-V_0}{\rho}+\frac{V_2-V_0}{\rho}+\frac{V_3-V_0}{\rho}+\frac{V_4-V_0}{\rho}+\frac{0-V_0}{R} = 0$$

which may be rewritten as

$$V_1+V_2+V_3+V_4-4V = \rho V_0/R. \tag{21}$$

Equations (20) and (21) are identical in ϕ and V if the resistances are chose such that

$$\rho/R = (\omega/U)^2 d^2.$$

When this condition is satisfied the network of resistors can be used to represent exactly the finite difference form of the differential equations and once the correct boundary conditions are set on the network it becomes a model of the mathematical idealisation of the problem.

For the particular case when $\omega h/U = 1$ and the tunnel height, is divided into eighty-eight mesh intervals ($h/d = 88$),

$$R = \rho(U/\omega d)^2 = \rho(88)^2,$$

where ρ is the standard mesh resistance of 100 ohms.

Since ϕ was required in greater detail in some regions, a system of graded meshes was used. By this means the mesh interval near to the wing and around the slots was made to equal $h/88$ whereas in regions where the change in ϕ was less rapid the interval was increased to $h/22$.

Of the boundary conditions which arise in the problem under consideration, that of the function, ϕ, taking known values can be satisfied directly by setting the equivalent voltage V to the nodes of the network. By doubling the value of the resistance on the boundaries, the condition of normal zero slope is automatically satisfied.

By using additional boundary-feeding resistors the condition (7) on a homogeneous boundary,

$$\phi+K\partial\phi/\partial n = 0,$$

can also be achieved automatically in the following manner. The slope at node 0 (Fig. 3a) can be written as

$$(\partial\phi/\partial z)_0 = (\phi_2-\phi_4)/2d,$$

but the homogeneous condition for the edge $z = \frac{1}{2}h$ is

$$\phi_0+K(\partial\phi/\partial z)_0 = 0.$$

Elimination of $(\partial\phi/\partial z)_0$ gives

$$\phi_2 = \phi_4-(2d/K)\phi_0.$$

When this is substituted in the finite difference form of the governing equation (20),

$$\phi_1+\phi_3+2\phi_4-4\phi_0 = (2d/K)\phi_0+(\omega/U)^2 d^2\phi_0. \tag{22}$$

If the circuit is modified with an extra resistor connected to each boundary node (Fig. 3c) the electrical equation becomes

$$V_1+V_3+2V_4-4V_0 = (2\rho/X)V_0+(\rho/R)V_0. \tag{23}$$

For the equations (22) and (23) to be analogous

$$2d/K = 2\rho/X \text{ or } X = (\rho/d)K.$$

As an example, the homogeneous condition where $a/l = 1/8$, $d/l = 1/16$ then

$$K = \frac{l}{\pi}\log_e \operatorname{cosec}(\pi a/2l) = \frac{l}{\pi}\log_e \operatorname{cosec}(\pi/16),$$

hence the resistance $X = \dfrac{16\rho}{\pi}\log_e \operatorname{cosec}(\pi/16)$ (24)

where the resistance ρ is 100 ohms.

The advantages of the resistance network method of solution are as follows:—

(1) In areas of particular interest the mesh interval can be decreased to permit a closer study of any critical effects.
(2) Only the values of the function in regions of particular interest need to be recorded.
(3) Boundary conditions can generally be applied automatically.
(4) Successive problems with the same geometry can be set on the network rapidly.

4. *Steady Flow in Slotted Wall Tunnels.*

The equation which has to be solved for the steady flow in slotted wall tunnels is the Laplace equation, $\nabla^2\phi = 0$. This equation is a standard problem for solution using a resistance network but techniques additional to the standard procedure are required to simulate the effect of discontinuities at the slots, to simulate the wing and also permit an accurate evaluation of the interference potential. Reference should also be made to the Appendix for a detailed treatment of the singularities.

4.1. *Discontinuities.*

Discontinuities in the slope of the velocity potential occur at the edges of the slats and so as to test the ability of the resistance network to simulate the flow around the edge of a slat, the first problem selected was one for which an analytical solution is available. This problem, the non-viscous flow through a grating, is discussed by Lamb[7]. The dimensions for the particular example studied here were chosen to approximate to the shape of the wind tunnel to be considered in the following section. The length was infinite, and breadth between the parallel walls 44 mesh intervals and the width of the slot 4 mesh intervals (so that the open area ratio was 1/11th); the total inflow set to be π units (Fig. 4a) and the boundary conditions are satisfied as described in Section 2.3. Appreciable errors were found to occur around the nodes representing the slot; the flow at the centre of the slot was found to be 15 per cent low and the flow at the quarter points of the slot was 18·5 per cent low.

These errors arose because the standard finite difference approximation is unable to represent the discontinuity in the slope of the velocity potential at the edge of the slot. To overcome this difficulty use can be made of additional information which is available about the form of the function around the singularity. The form of the velocity potential around the edge of an obstacle consisting of a thin wall in an infinite field is known, and since the shape of the function sufficiently close to the edge of the wall does not depend on the remainder of the field, this information can be used in the finite difference analysis of any

problem in which the flow is restricted by a thin wall, whatever the other boundary conditions.

However, the magnitude of the function is dependent on the remainder of the field and therefore a mathematical solution is used close to the singularity, the standard finite difference solution is used in the remainder of the field and these two solutions are made to join smoothly.

The flows close to the edge of the wall takes the form,

$$\phi = A_1 r^{\frac{1}{2}} \sin\theta/2 + A_2 r^{3/2} \sin 3\theta/2 + \ldots \tag{25}$$

where A_1 and A_2 are unknown constants,

r is the radius from the edge of the wall,

θ is the angle of the radius measured from the line across the open portion of the slots (Fig. 4b).

At the four points C, D, E, F, surrounding the edge of the wall as shown in Fig. 4b, the expressions for the functions ϕ are:

$$\phi_C = A_1 h^{\frac{1}{2}} \sin\pi/2 + A_2 h^{3/2} \sin 3\pi/2$$

$$\phi_D = A_1 (2h)^{\frac{1}{2}} \sin\pi/2 + A_2 (2h)^{3/2} \sin 3\pi/2$$

$$\phi_E = A_1 h^{\frac{1}{2}} \sin\pi/4 + A_2 h^{3/2} \sin 3\pi/4$$

$$\phi_F = A_1 (2h)^{\frac{1}{2}} \sin\pi/4 + A_2 (2h)^{3/2} \sin 3\pi/4.$$

By eliminating A_1 and A_2 the functions ϕ_C and ϕ_E can be written in terms of ϕ_F and ϕ_D,

$$\left.\begin{aligned} \phi_C &= 0{\cdot}25\phi_F + 0{\cdot}5303\phi_D \\ \phi_E &= 0{\cdot}5303\phi_F + 0{\cdot}125\phi_D \end{aligned}\right\} \tag{26}$$

In order to ensure that this particular function joins smoothly with the normal resistance solution, an iterative procedure has to be adopted. From an initial solution in which the normal resistance network is used over the entire field, values of ϕ_D and ϕ_F are measured and from substitution in equations (26) values of ϕ_C and ϕ_E are calculated. These are set as potentials on the network, and new values of ϕ_D and ϕ_F are measured. This process is repeated until the calculated values of ϕ_C and ϕ_E equal those set in the previous iteration. When this occurs both the special formula and the standard finite difference equations are satisfied in the region between BEC and AFD.

When the solution of the flow through the gating was repeated by use of the special singularity function, the values of the flow across the slot agreed more closely with the analytical values of Lamb, the greatest error being 3 per cent, a satisfactory result for such a coarse net. The total flow $\left[\int \frac{\partial\phi}{\partial z} dy\right]_{z=\text{const}}$ is defined as π and the localised flow $d\,(\partial\phi/\partial z)$ for points A and B (Fig. 4) tabulated below.

	Point A	Point B
Exact solution	0·524	0·598
Standard resistance network solution	0·445	0·487
Solution with singularity formula	0·540	0·611

4.2. *Simulation of the Wing.*

In this study the wing could be assumed to be either elliptically loaded or uniformly loaded. However, when the span of the wing tends to zero, these two loading cases become the same, and the unconstrained velocity potential for $\omega \to 0$ is

$$\phi_m = \frac{USC_L}{4\pi} \frac{z}{r^2}. \tag{27}$$

In view of the singularity at the origin it is clear that ϕ cannot be set at this point of the resistance network. However, if it is permissible to represent the wing by setting values on an arc enclosing the point wing, the difficulty would be overcome. For example, with an arc of radius approximately $h/12$, the values of ϕ_m on the Z axis is about ten times the largest value of ϕ on the roof of the tunnel. Such a range of values can easily be set on the resistance network.

To verify that there is no finite difference error when simulating the wing of small span by setting the function on a small arc around the origin, the following experiment was performed. A large field was divided into a square mesh and values of ϕ_m, calculated according to equation (27) were set both on an arc a short distance from the origin and on the external boundary of the field. Potentials throughout the field were measured and were found to agree everywhere with calculated values of ϕ_m. If the setting of the function on the arc had been inadequate, discrepancies between the values would have occurred within the field, from the close agreement it was assumed that the simulation is satisfactory.

4.3. *Determination of Interference Potential.*

When carrying out the analysis the quantities which have to be determined accurately are,

(a) the total flow towards each slot;

(b) the interference potential at the wing.

These two quantities were determined in the following manner. The total flow, Q, through a slot in the plane of the model (which equals half the value at infinity) was calculated from

$$2\mathrm{Q} = \int \frac{\partial \phi}{\partial z} dy,$$

$$\text{or } \frac{8\pi h Q}{USC_L} = \frac{1}{F'} \int \frac{\partial V}{\partial z} dy.$$

In practice integration was taken across a rectangular boundary approximately six mesh intervals from the slot.

The lift interference parameter for a small model, δ_0 is determined from the expression,

$$2\delta_0 = \frac{bh}{USC_L} \left(\frac{\partial \phi_i}{\partial z} \right)_0;$$

again the parameter is evaluated in the plane of the model. The term $(\partial \phi_i / \partial z)_0$ is calculated by numerical differentiation using a three point formula.

Two methods of determining the interference potentials were studied, in the first a single solution in terms of the interference potential only was obtained, whereas in the second method successive solutions in the velocity potential and then the interference potential were tried until convergence occurred.

4.3.1. *First method.*

For the first attempt the analysis of the flow in the tunnel was only in terms of the interference potential where $\phi_i = \phi - \phi_m$. Since an analytical expression is available for ϕ_m and the boundary conditions were stated in terms of ϕ, the problem can be stated entirely in terms of ϕ_i. The governing equation to be solved is

$$\frac{\partial^2 \phi_i}{\partial y^2} + \frac{\partial^2 \phi_i}{\partial z^2} = 0 \text{ for } |y| < \tfrac{1}{2}b, \; |z| < \tfrac{1}{2}h, \tag{29}$$

with $\partial\phi_i/\partial y = -\partial\phi_m/\partial y$ on $y = \pm\frac{1}{2}b$ (because the flow across the vertical walls of the tunnel $\partial\phi/\partial y$ is zero),

$\partial\phi_i/\partial z = -\partial\phi_m/\partial z$ on $z = \pm\frac{1}{2}h$ for the closed portions of the roof and floor (because the flow across the closed portion of the roof $\partial\phi/\partial z$ is zero),

$\phi_i = -\phi_m$ on $z = \pm\frac{1}{2}h$ for the open portions of the roof and floor (because the value of ϕ across the slots is zero),

$\phi_i = 0$ on $z = 0$ on the horizontal centre line.

The advantage of working directly in terms of ϕ_i is that the interference upwash $\partial\phi_i/\partial z$ at the wing is a small quantity which can be evaluated directly, whereas if it was calculated from an experiment in ϕ, being a small quantity compared with $\partial\phi/\partial z$ and $\partial\phi_m/\partial z$ it would be liable to error.

However considerable practical difficulty was encountered in setting the boundary slopes $\partial\phi_i/\partial y$ and $\partial\phi_i/\partial z$. Further, a very severe variation of the function ϕ_i occurs in the neighbourhood of the slots with the result that it was virtually impossible to satisfy the boundary conditions in that region. Thus, through reliable values of the interference potential remote from the slots were obtained, the solution could not be used to determine accurately values of the flow at the slots.

4.3.2. *Second method.*

As an alternative to only working in terms of ϕ_i, a step by step procedure was carried out whereby successive experiments in ϕ and ϕ_i quickly led to solutions giving all necessary results.

In carrying out the first analysis in terms of ϕ the boundary conditions can be stated as,

$\partial\phi/\partial n = 0$ on closed portions of the tunnel wall and roof and $y = 0$

$\phi = 0$ on open portions of the tunnel roof and $z = 0$

with the wing simulated as in the manner of Section 4.2. For the initial experiment it is necessary to set values of ϕ_m (the velocity potential in an unrestricted field) on the arc around the wing. But, because the velocity potential will be modified due to the interference effects of the tunnel boundary, in a later experiment the velocity potential on the arc is set from $\phi = \phi_m + \phi_i$.

Therefore the procedure is that an experiment in ϕ is carried out with the correct conditions on the tunnel boundaries but with calculated values of ϕ_m set around the wing. This is followed by an experiment in ϕ_i on the same resistance network with the potentials at the boundary of the tunnel calculated from $\phi_i = \phi - \phi_m$ and with the condition that $\phi_i = 0$ on the line $y = 0$.

The third experiment involves a repeat of the analysis in ϕ but with corrected values on the arc around the wing. In the final experiment new calculated values of ϕ_i are applied on the boundary. Provided that the values of ϕ_i in this last experiment have changed little from the second experiment it can be assumed that convergence has occurred. The four steps are summarised in Fig. 5.

In the experiments in ϕ the singularity formula was used, and since ϕ_i was set from $\phi_i = \phi - \phi_m$ the singularity formula was implicit in the experiments in ϕ_i. However, it was necessary to calculate the set values of ϕ_i not only on the tunnel boundaries but also on the nodes within the tunnel where singularity potentials in ϕ had already been applied.

5. *Experiments in Steady Flow.*

The particular tunnel represented on the electrical analogue has a height/breadth ratio of one half with the wing in the centre of the tunnel. To represent the conditions in the N.P.L. slotted wall tunnels the open area ratio a/l is taken to be 1/11 (Table 1 of Ref. 1). Four slots were taken in both the roof and floor, and in the first experiment a slot is positioned directly above the model and a half slot is adjacent to each side wall. Due to symmetry only one quarter of the tunnel need be studied.

5.1. *Exploratory Work.*

Exploratory tests were conducted with a uniform square mesh the full breadth of the tunnel being represented by 88 mesh intervals, and each slot by 2 mesh intervals. Potentials on the arc around the wing were set by using ten turn helical potentiometers, the maximum potential being 2 volts. Values equivalent to ϕ_i were set on the tunnel boundaries by means of potential dividers, which consist of a length of resistance wire with numerous tappings. Measurement of the potentials was achieved either through a digital voltmeter or by a null method using a voltage dividing resistance.

With this tunnel singularities occurred on the edges of each slot, but by following the procedure described in Section 4.1 adjustments were carried out simultaneously at all the singularities and rapid convergence occurred.

5.2. *Solutions with Finer Net.*

Though the results of the exploratory tests appeared to be satisfactory, it was thought to be advisable to halve the mesh size in the regions around the slots and the wing. Therefore a graded network was introduced and the form of the grading can be seen from the mesh numbering on the results sheet, Fig. 7. A photograph of the apparatus and ancillary equipment is included in Fig. 6. In the first experiment when ϕ_m was set around the wing, the magnitude for the point where the arc crosses the z axis was 10000 but it had to be corrected due to the tunnel interference to 9943 for the third experiment. However, little change was noted in the values of ϕ_i between the second and fourth experiments.

It is not possible to assess directly the accuracy of either the coarse net or the graded net, since there is no exact theory with which the results can be compared. However the close agreement between the potentials in the two experiments suggests that there is no serious net effect. In particular the comparison of the flow through the individual slots, to be found in the following table, indicates that the finite net is a satisfactory representation of the flow within the tunnel.

Position of slot	Flow $\frac{USC_L}{4\pi h}$	
	176×88 graded net	88×44 uniform net
$y = 0, \quad z = \frac{1}{2}h$	+2·30	+2·36
$y = \frac{1}{2}h, \quad z = \frac{1}{2}h$	+0·72	+0·73
$y = h, \quad z = \frac{1}{2}h$	+0·08	+0·085

5.3. *Slot and Slat Centres Interchanged.*

In a second experiment the slot and slat centres were interchanged such that there was a slat directly above the wing. The experiment was carried out on the 88×44 network and the flows calculated as before.

The flows through the individual slots were $+1{\cdot}60$ and $+0{\cdot}225 \times 4\pi h/USC_L$. A comparison showing the effect on the interference upwash of interchanging the slots and slats is to be found in the table included in the following section. The total flow through the slots is reduced from $\sum 8\pi hQ/USC_L = 3{\cdot}90$ to 3·79 for the case where a slat is directly above the model.

5.4. *Homogeneous Boundary Condition.*

Little modification is required to the experimental technique to permit the setting of the homogeneous condition,

$$\phi + K\,\partial\phi/\partial z = 0$$

on the tunnel roof and floor. Resistors, calculated according to Section 3 are connected from the boundary nodes on the tunnel roof to zero potential, whilst the tunnel sides are left free thus satisfying the condition $\partial\phi/\partial n = 0$. The first analysis in ϕ is carried out as before with the values of ϕ_m applied on the arc around the wing. From this solution values of ϕ_i are calculated for the tunnel wall and roof, and an analysis in ϕ_i is performed. This is followed by a further experiment in ϕ with improved values set around the wing and a final experiment in ϕ_i leads to the required information about the interference upwash.

In the following table the exact solution for the interference upwash (Reference 3) is compared with the results for the homogeneous condition and the slotted tunnels.

	δ_0
Homogeneous boundary (exact solution)	−0·0871
Homogeneous boundary (Analogue solution)	−0·0869
Slotted tunnel, slot above wing	−0·0976
Slotted tunnel, slat above wing	−0·0642

6.0. *Unsteady Flow.*

The resistance network technique can readily be extended to include the effect of unsteady flow. The governing equation,

$$\frac{\partial^2\phi}{\partial y^2} + \frac{\partial^2\phi}{\partial z^2} = (\omega/U)^2\phi, \tag{5}$$

can be analysed on a resistance network constructed according to Section 3.

The range of frequency parameters analysed was such that

$$0 \leqslant \omega h/U \leqslant 1$$

and the actual values studied were $\omega h/U = 0$, 0·1988, 0·5101 and 1·000. There is no special significance in the magnitude of the values chosen; they were selected to coincide with standard resistance values. For a mesh resistance of 100 ohms, the resistances used to simulate the frequency parameter corresponding to a unit mesh were $20M$ ohms, $3M$ ohms and $774K$ ohms. In the photograph of the apparatus, Fig. 6, the mesh resistors are mounted in the horizontal board, and the resistors corresponding to the frequency are set in the vertical board.

In order to satisfy the singularity condition on the edge of the slots, a technique similar to that used in steady flow is adopted. The general form of the singularity equations is derived in the Appendix and for the particular frequency parameter $\omega h/U = 1{\cdot}0$ they become,

$$\phi_C = 0{\cdot}24997\,\phi_F + 0{\cdot}53030\,\phi_D$$

$$\phi_E = 0{\cdot}53030\,\phi_F + 0{\cdot}12499\,\phi_D$$

These coefficients are so close to those used for steady flow in equation (26), that it is sufficiently accurate to use the steady state equations for all the frequency values considered in this report.

A similar system of iteration was adopted working first in ϕ and then in ϕ_i also the scale factor remained unchanged from that given in Section 2.4. From the resultant values of ϕ and ϕ_i the total flow towards the slots and the interference upwash at the origin were determined. The manner in which these depend on the frequency is illustrated by the graphs of Fig. 8.

7. *Concluding Remarks.*

In this report a pure resistance electrical network has been described which represents a two dimensional perturbation velocity potential over the cross section of a slotted rectangular wind tunnel. Though the use of a network implies that the field is divided into a finite mesh, by the introduction of graded nets sufficient detail is obtained in regions where the change in potential is rapid. Additional techniques have been devised to cope with the singular behaviour at the small wing and also on the edges of the slots.

Using the resistance network, information has been obtained about the interference upwash parameter at the origin of the wing in steady flow. The experimental value with the homogeneous condition on the boundary is found to agree well with the analytical value from Ref. 3. The values for actual slots, with the slot or the slat above the wing, are found to lie on either side of the homogeneous condition. It is physically reasonable that the case where the slot is positioned above the origin should deviate towards that of an open tunnel, while the case with a central slat should tend towards the closed boundary condition.

A second important conclusion which can be deduced from the results of this report is that the magnitude of the inflow near the roof slots tends to be reduced as the frequency of the oscillation increases. A more accurate simulation of the conditions with a free stream surface bridging each slot would be advantageous, but it would require a much finer grid in the neighbourhood of the slots with an iterative process on the boundary even in steady flow. Under such conditions the tunnel boundaries, would no longer be cylindrical, so that the present approach would not apply. The time dependent free boundaries of an oscillatory flow in a slotted tunnel could still provide a clue to the large interference effects observed in slotted tunnels (Ref. 1).

Further work which is being carried out with the two dimensional resistance network includes the effect of increasing the number of slots in the roof of the tunnel and determining how the interference parameter converges to the analytical results of the homogeneous condition. Another problem being studied is that of all four walls slotted.

The success of the two dimensional network suggests that a three dimensional network would be useful, for it would permit the evaluation of the streamline curvature correction for slotted tunnels. It might also be applied to the more difficult problem of interference upwash near an oscillating model.

8. *Acknowledgement.*

This report describes the initial investigations for the study of wind tunnel interference effects by means of an analogue computer.

The study of these wind tunnel interference problems was suggested by Mr. H. C. Garner of the National Physical Laboratory, and the mathematical derivations in Section 2 are based on his notes. The author wishes to thank him and his colleagues for all their help.

Also the author wishes to acknowledge the help given by Miss G. Vaisey on the theoretical aspects of the study and by Miss L. Laing who carried out the experimental work.

NOTATION

A_1, A_2	Arbitrary constants
a	Width of slot
b	Tunnel breadth
C_L	Lift coefficient
d	Mesh interval
F'	Scaling factor
h	Height of tunnel
I_n, K_n	Bessel functions ($n = \frac{1}{2}, 1, \ldots$)
K	Geometric slot parameter equation (7)
l	Periodic slot spacing
M	Mach number
R, ρ	Resistances
r	Radial co-ordinate
S	Planform area
s	Semi-span of wing
t	Time
U	Undisturbed stream velocity
u,v,w	Velocity components
V	Voltage
X	Resistance
x,y,z	Co-ordinates
θ	Angle
ρ	Stream density
δ_0	Lift interference parameter for small model
Φ	Perturbation velocity potential
$\bar{\phi}$	Φ = Real part of $(\bar{\phi}(x,y,z)e^{i\omega t})$
$\phi(y,z)$	Two-dimensional velocity potential in equation (4)
$\Phi_m\, \phi_m$	Φ,ϕ for model in unconstrained flow
$\Phi_i\, \phi_i$	Interference velocity potential
ω	Angular frequency of the oscillation

REFERENCES

No.	*Author(s)*	*Title, etc.*
1	K. C. Wight	A review of slotted wall wing tunnel interference effects on oscillating models in subsonic and transonic flow. *J.R. Ae. Soc.* Vol. 66, 1964, pp. 670 – 674.
2	H. Glauert	Wind tunnel interference on wings, bodies and airscrew. R. and M. 1566. Sept., 1933.
3	D. D. Davis Jun and D. Moore ..	Analytical study of blockage- and lift-interference corrections for slotted tunnels obtained by the substitution of an equivalent homogeneous boundary for the discrete slots. NACA RM L53E07b (NACA/TIB/3792). June, 1953.
4	L. Howarth	*Modern Developments in Fluid Dynamics. High Speed Flow.* Clarendon Press, 1953. Chapter 9.
5	G. Liebmann	Electrical Analogues. *Brit. Jnl. Appl. Phys.* Vol. 4. February, 1955, p. 13.
6	S. C. Redshaw	Use of an electrical analogue for the solution of a variety of torsion problems. *Brit. Jnl. Appl. Phys.* Vol. 11. Oct., 1960. p.461.
7	H. Lamb	*Hydrodynamics.* Cambridge University Press. 6th edition, 1932. pp. 533 – 535.

APPENDIX

Singularity Equations.

The need to introduce singularity equations arises from the inability of the standard finite difference network to represent the infinite slope of the function which occurs at the edge of the slot. If the normal finite difference expansion is replaced by an alternative expression in the neighbourhood of the slot, such that this alternative expression satisfies the condition of infinite slope, then an improved solution can be anticipated.

The following derivation was suggested by Mr. W. E. A. Acum of the National Physical Laboratory, but the originator of this method is not known.

Within the region R bounded by the closed curve C, Fig. A1, the governing equation is equation (5), and the boundary conditions are that ϕ vanishes on $0P$ and its normal derivative vanishes on $0Q$. It is convenient to write equation (5) in polar form,

$$\frac{\partial^2\phi}{\partial r^2}+\frac{1}{r}\frac{\partial\phi}{\partial r}+\frac{1}{r^2}\frac{\partial^2\phi}{\partial\theta^2}-\left(\frac{\omega}{U}\right)^2\phi=0; \tag{A1}$$

the corresponding boundary conditions are,

$$\phi = 0 \text{ on } \theta = 0,$$

$$\partial\phi/\partial\theta = 0 \text{ on } \theta = \pi. \tag{A2}$$

The general solution of equation (A1) and the boundary conditions are given by the infinite series

$$\phi = \sum_{m=1}^{\infty}\left[A_m I_{m-\frac{1}{2}}(\omega r/U)+B_m K_{m-\frac{1}{2}}(\omega r/U)\right]\sin(m-\tfrac{1}{2})\theta, \tag{A3}$$

where I_m and K_m are Bessel Functions and A_m and B_m are constants. But K_m has an infinity at $r = 0$ and must be rejected to keep ϕ finite. Hence

$$\phi = \sum_{m=1}^{\infty} A_m I_{m-\frac{1}{2}}(\omega r/U)\sin(m-\tfrac{1}{2})\theta. \tag{A4}$$

If $\phi = g(\theta)$ is known on any small circle $r = r_0$, the constants A_m can be evaluated.

However, ϕ may be expanded in the form of (A4) and close to 0 it is sufficient to take only the first two terms of the expansion. Then the expressions for the points C, D, E, and F, Fig. 4b, can be written in terms of the two constants A_1 and A_2. For example,

$$\phi_c = A_1 I_{1/2}(\omega d/U)\sin\pi/2+A_2 I_{3/2}(\omega d/U)\sin 3\pi/2$$

and there are similar expressions for ϕ_D,ϕ_E and ϕ_F. Elimination of $A_1$and A_2 gives,

$$\begin{aligned}\phi_C &= \tfrac{1}{2}\alpha\,\phi_D+\frac{\sqrt{2}}{2}\beta\phi_F,\\ \phi_E &= \frac{1}{2\sqrt{2}}\beta\phi_D+\tfrac{1}{2}\alpha\,\phi_F,\end{aligned} \tag{A5}$$

where

$$\alpha = \frac{I_{1/2}(\omega\, d/U)}{I_{1/2}(2\omega\, d/U)} + \frac{I_{3/2}(\omega\, d/U)}{I_{3/2}(2\omega\, d/U)}$$

$$\beta = \frac{I_{1/2}(\omega\, d/U)}{I_{1/2}(2\omega\, d/U)} - \frac{I_{3/2}(\omega\, d/U)}{I_{3/2}(2\omega\, d/U)}. \tag{A6}$$

Equation (A5) reduces to equation (26) when $\omega \to 0$.

The manner in which these equations are used in a resistance network solution is described in Section 4.1.

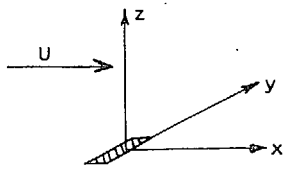

FIG. 1. Orientation of axes.

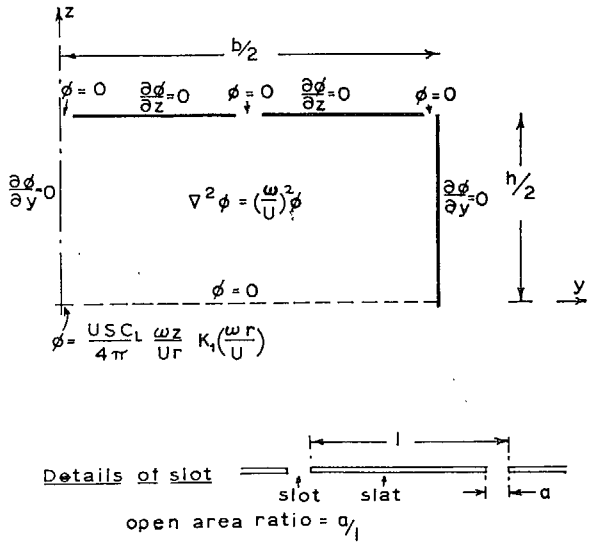

FIG. 2. Two-dimensional problem in plane x = infinity

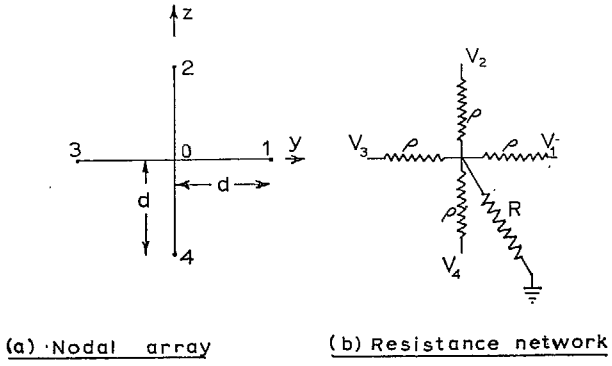

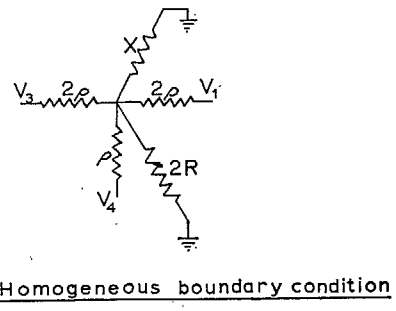

FIG. 3. The resistance network

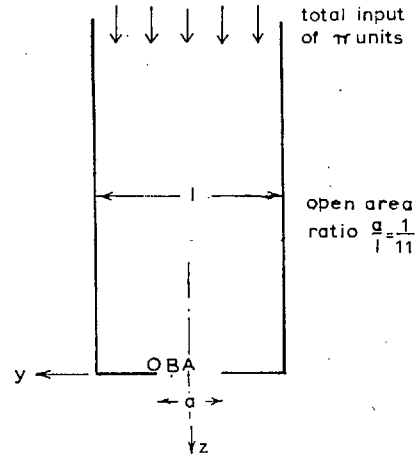

(a) Geometry of flow

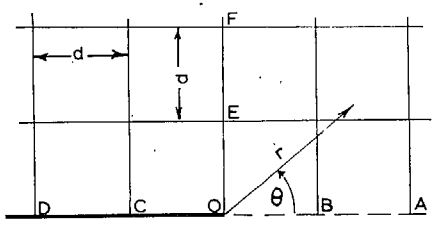

(b) Treatment of singularity at edge

FIG. 4. Flow through grating

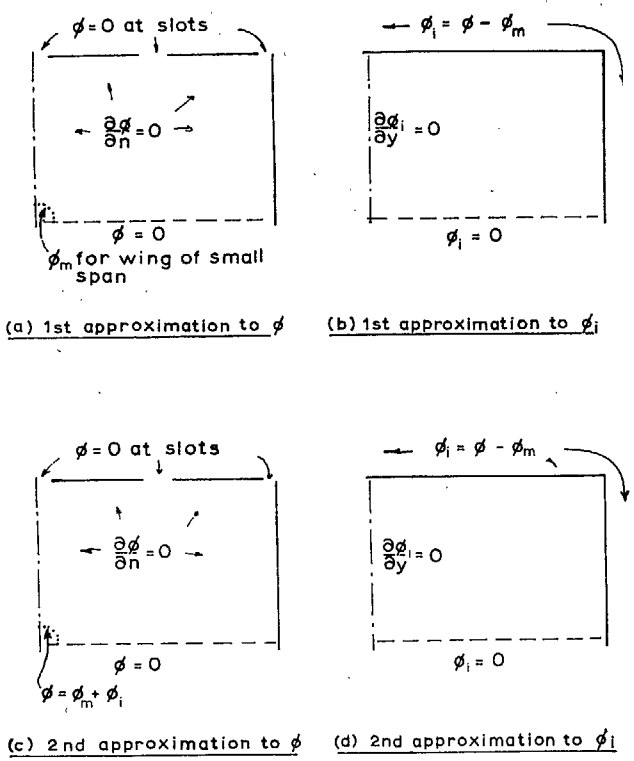

(a) 1st approximation to ϕ (b) 1st approximation to ϕ_i

(c) 2nd approximation to ϕ (d) 2nd approximation to ϕ_i

FIG. 5. Sequence of experiments to determine ϕ and ϕ_i

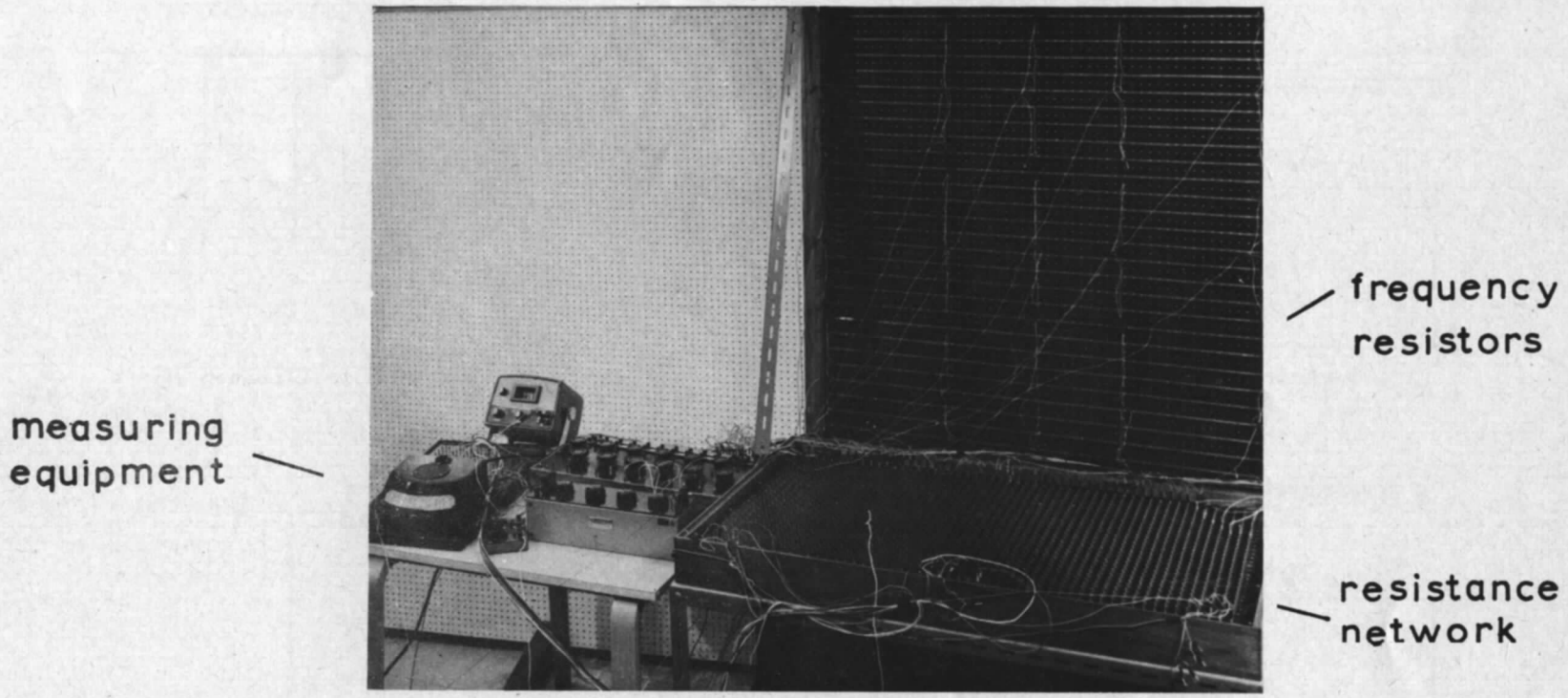

FIG. 6. Electrical network

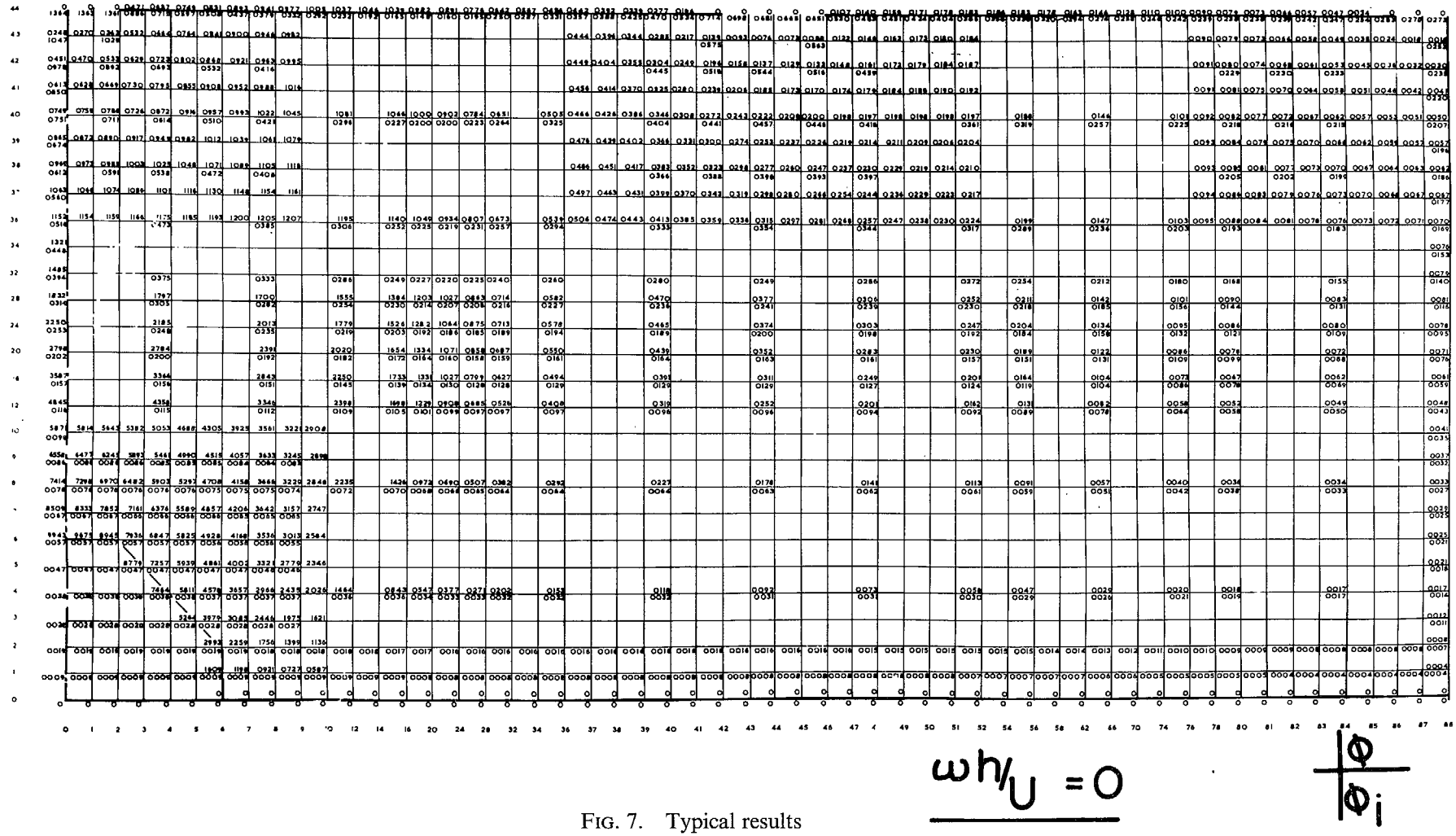

FIG. 7. Typical results

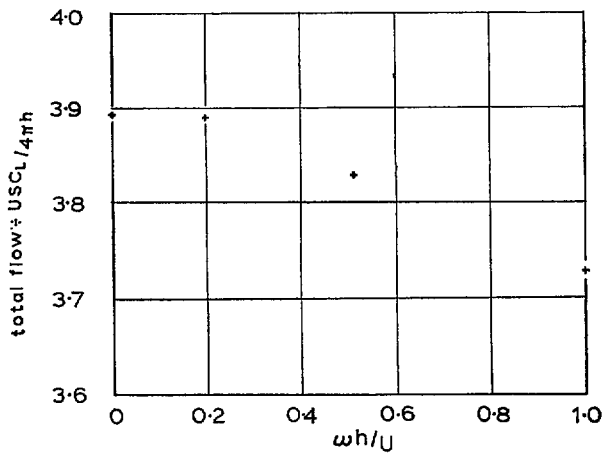

(a) Total flow through slots

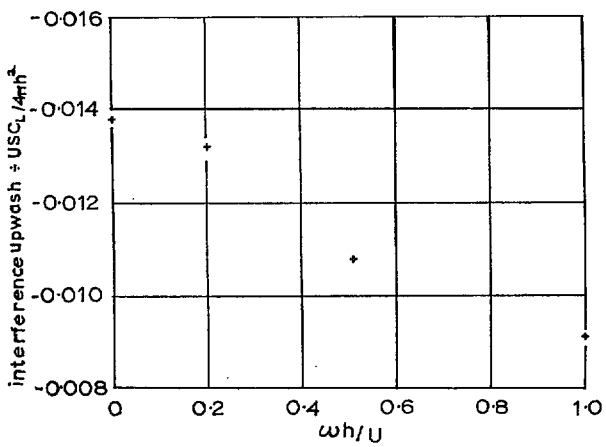

(b) Interference upwash at tunnel centre

FIG. 8. Effect of frequency parameter in distant wake

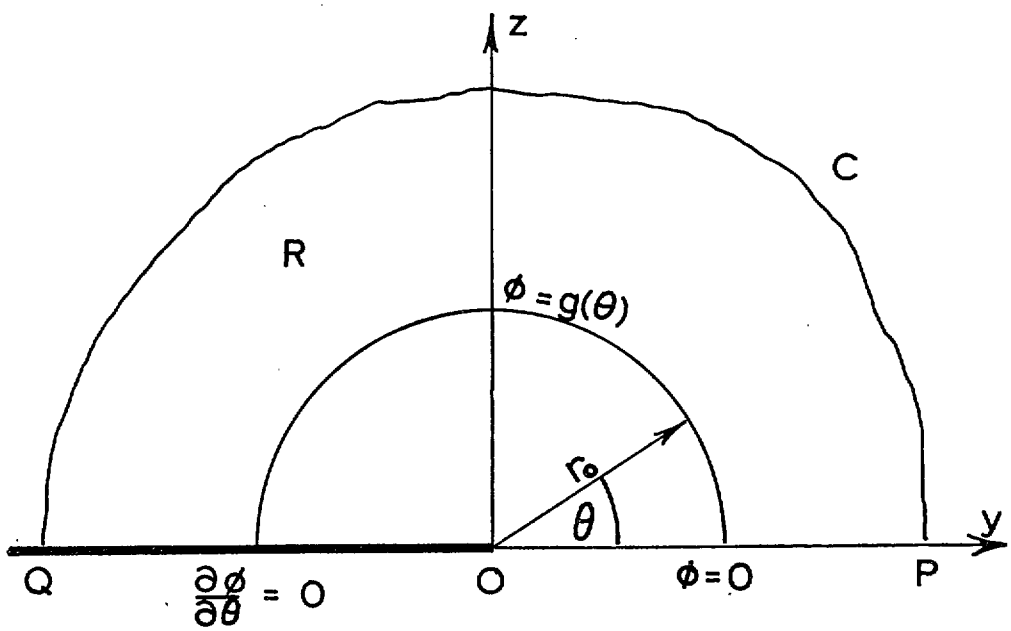

FIG. A1. Singularity formula

Part II.—Particular Examples of Slotted-Wall Tunnel Interference in Steady Flow

Summary.

In Part II the electrical analogue computer is used to obtain results for two particular steady flow problems. The first involves a comparison between actual slotted walls and an equivalent homogeneous condition. In the second the lift interference for tunnels with all four walls slotted is examined.

1. *Introduction.*

Part I describes an electrical analogue computer which can be used to investigate the interference velocity potential in slotted wind tunnels. The computer consists of a rectangular array of resistors which form, in effect, a model of the tunnel. The equations of the electrical network are made identical to the finite difference form of the two-dimensional differential equation which governs the linearized flow in the wake of an oscillating wing.

The resistance network is now used to estimate the interference upwash in steady flow for two types of tunnel boundary. The first study is concerned with small lifting wings in rectangular tunnels with both the roof and the floor slotted. As the number of slots is increased from two, the interference upwash for discrete slots converges towards that for an equivalent homogeneous condition, and conclusions can be made concerning the adequacy of the homogeneous condition.

Secondly rectangular tunnels with slots on each wall were investigated. Three typical shapes of tunnel were examined with homogeneous conditions ranging from open to closed boundaries.

2. *Résume of the Analogue Method.*

A detailed derivation of the governing equations and the analogy between the physical and electrical system has been given by the author in Part I, but in this Section a brief résumé will be given of the information relevant to the present studies.

For steady subsonic flow in a cylindrical tunnel of infinite length the perturbation velocity potential, ϕ, in the transverse plane of a small model is governed by the Laplace equation.

$$\partial^2\phi/\partial y^2 + \partial^2\phi/\partial z^2 = 0. \tag{1}$$

If a lifting wing of small span is positioned on the axis of the tunnel, the velocity potential in the plane of the wing is

$$\phi_m = \frac{USC_L}{8\pi}\,\frac{z}{r^2} \tag{2}$$

where U is the undisturbed stream velocity, S is the planform area, C_L is the lift coefficient, z and r are the vertical and radial distances from the wing.

Various linearized conditions can occur on the walls of the tunnel. On an open boundary, or a slot, $\phi = 0$, and on a closed boundary or a slat $\partial\phi/\partial n = 0$. Instead of treating a slotted boundary as separate slots and slats an equivalent homogeneous condition can be used

$$\phi + K\,\partial\phi/\partial n = 0, \tag{3}$$

where

$$K = \frac{1}{2}Fh = \frac{l}{\pi}\log_e \operatorname{cosec}\frac{\pi a}{2l} \tag{4}$$

is a constant dependent on the open area ratio, a/l, and the slot spacing l. The object to determine the interference effects, is most conveniently achieved by an analysis in ϕ followed by a further analysis in the interference potential ϕ_i,

$$\phi_i = \phi - \phi_m.$$

This satisfies the Laplace equation subject to the boundary values equal to the difference between an initial value of ϕ, and the calculated values ϕ_m for an unconstrained field.

The resistance network automatically solves the finite difference form of the Laplace equation (1), and the boundary conditions are applied as voltages or currents. Then electrical potentials are measured on the network and these are equivalent to the velocity potentials. For further details of the analogue techniques reference should be made to Section 3 of Part I. Finally the interference upwash at the wing is expressed as a lift interference parameter

$$\delta_0 = \frac{hb}{USC_L} \frac{\partial \phi_i}{\partial z}. \tag{6}$$

3. *Validity of the Equivalent Homogeneous Condition.*

The validity of the equivalent homogeneous boundary condition (3) was investigated by considering a duplex tunnel ($h/b = 0{\cdot}5$) having solid side walls, but slotted roof and floor of open area ratio $a/l = 0{\cdot}125$. Two symmetrical arrangements of the slots are possible; either a slot or a slat is positioned centrally above and below the wing. Four cases of each arrangement were considered, with two, three, four and six complete slots, as illustrated in Fig. 1. At the edges of the slots discontinuities in the slope of the potential occur, and care must be taken to ensure that these critical regions are represented adequately by the resistance network. The singularities were treated using the method of Section 4.1 of Part 1, and the mesh interval was chosen so that each complete slot was represented by two mesh intervals. Hence for the tunnel with two slots the width of the tunnel was represented by 32 mesh intervals, but for the tunnel with six slots, 96 intervals were required.

The homogeneous boundary condition varies according to the number of slots through the parameter l/h. In one instance, when there were four complete slots, the analysis was performed with a central slot, with a central slat and also with the equivalent homogeneous condition set on the tunnel roof. The lift interference parameters were respectively $\delta_0 = -0{\cdot}122$, $-0{\cdot}091$ and $-0{\cdot}1032$. An analytical expression (6) for δ_0 with the homogeneous condition leads to a value of $\delta_0 = -0{\cdot}1044$ which confirms the estimated accuracy of ± 2 per cent or better. Values of δ_0 from the electrical analogue together with the analytical values based on the equivalent homogeneous condition, are recorded in Table I and are plotted in Fig. 2 against $(1+F)^{-1}$ from equation (4). The closed and open tunnels, $(1+F)^{-1} = 0$ and $1{\cdot}0$ respectively, are the two extreme conditions.

Fig. 2 suggests that for more than four slots the lift interference effects at the wing are satisfactorily represented by the equivalent homogeneous condition. However, if there are three or fewer slots there are large differences between the three values of δ_0. It will be noted that the boundary immediately above and below the wing is significant; the correct result with a central slat deviates towards that for a closed tunnel, while the central slot gives more open (i.e. more negative) lift interference than that predicted by the homogeneous condition. For six slots, however, with central slot or central slat, δ_0, instead of stradling the homogeneous value, slightly less in both cases, but the difference is within the estimated order of accuracy of the analogue technique.

Thus for more than four slots the equivalent homogeneous boundary condition can be expected to apply to practical slot arrangements, provided that viscous effects can be ignored.

4. *Rectangular Tunnel with Four Walls Slotted.*

Davies and Moore[1] derive the interference parameter δ_0 for small wings in rectangular tunnels with four walls slotted by transforming the velocity potential for a uniformly slotted circular tunnel. Unfortun-

ately the rectangular tunnels do not remain uniformly slotted, and no analytical solutions are available for four uniformly slotted walls. Therefore analogue solutions have been obtained for the lift interference parameter over the practical range of rectangular tunnels with the equivalent homogeneous condition set on each wall. Table 2 gives δ_0 for small wings in three shapes of tunnel ($h/b = 0{\cdot}5$, $1{\cdot}0$ and $1{\cdot}6$) with five slot conditions $(1+F)^{-1} = 0$, $0{\cdot}35$, $0{\cdot}65$, $0{\cdot}85$ and 1.

The analytical values in the right-hand column of Table 2 are calculated from the appropriate formula in Ref. 2 for open and closed tunnels. These are seen to be in good agreement with the end values from the electrical analogue. The three curves of δ_0 against $(1+F)^{-1}$ are shown in Fig. 3. These are very roughly linear in $(1+F)^{-1}$, as is exactly true for small wings in multi-slotted circular tunnels (Ref. 2), and in rectangular tunnels having very small or very large ratios h/b. Nevertheless, Fig. 3 shows that small errors would result if a strictly linear variation were assumed between the exact limits of open and closed tunnels.

5. *Concluding Remark.*

In this report a pure resistance analogue computer has been used to calculate detailed results for the lift interference in slotted wall wind tunnels with small models in linearized potential flow. The results are estimated to be within ± 2 per cent, an accuracy which is adequate since the mathematical idealisation used in this analysis differs from the actual working of a tunnel; viscous and other non-linear effects at the slotted boundaries must contribute major uncertainties. Treatment of these effects requires on the one hand empirical data concerning slot flow, and on the other a three dimensional network.

NOTATION

a	Slot width
b	Tunnel breadth
C_L	Lift coefficient, lift/$\frac{1}{2}\rho U^2 S$
l	Periodic slot spacing
F	Non-dimensional slot parameter
h	Tunnel height
K	Geometric slot parameter
n	Outward normal
r	Radial ordinate
S	Planform area
U	Undisturbed stream velocity
y, z	Coordinates in transverse plane
δ_0	Lift interference parameter
ρ	Air density
ϕ	Velocity potential in transverse plane
ϕ_i	Interference velocity potential
ϕ_m	Unconstrained velocity potential

REFERENCES

No.	*Author(s)*	*Title, etc.*
1	D. D. Davis and D. Moore . .	Analytical study of blockage – and lift interference corrections for slotted tunnels obtained by the substitution of an equivalent homogeneous boundary for the discrete slots. NACA RM, L53E076. June, 1953.
2	T. Theodorsen	The theory of wing-tunnel wall interference. NACA Report 410. 1931.

TABLE I

Duplex Tunnel With Slotted Roof and Floor

Number of slots	F	$(1+F)^{-1}$	δ_0			
			Electrical Analogue			Analytical
			Slot above wing	Slat above wing	homogeneous condition	homogeneous condition
0	∞	0	—	—	+0·138	+0·137
2	1·040	0·490	−0·303	+0·098	—	−0·038
3	0·694	0·591	−0·106	−0·041	—	−0·077
4	0·520	0·658	−0·122	−0·091	−0·103	−0·104
6	0·347	0·743	−0·151	−0·145	—	−0·141
∞	0	1·0	—	—	−0·262	−0·262

TABLE 2

Rectangular Tunnels with Homogeneous Conditions on all Four Walls

$h/b = 0{\cdot}5$

$(1+F)^{-1}$	δ_0	
	Analogue	Analytical
0	+0·130	+0·137
0·35	+0·008	—
0·65	−0·108	—
0·85	−0·193	—
1·0	−0·263	−0·262

$h/d = 1{\cdot}0$

$(1+F)^{-1}$	δ_0	
	Analogue	Analytical
0	+0·137	+0·137
0·35	+0·027	—
0·65	−0·051	—
0·85	−0·099	—
1·0	−0·136	−0·137

$h/b = 1{\cdot}6$

$(1+F)^{-1}$	δ_0	
	Analogue	Analytical
0	+0·212	+0·210
0·35	+0·069	—
0·65	−0·023	—
0·85	−0·078	—
1·0	−0·122	−0·121

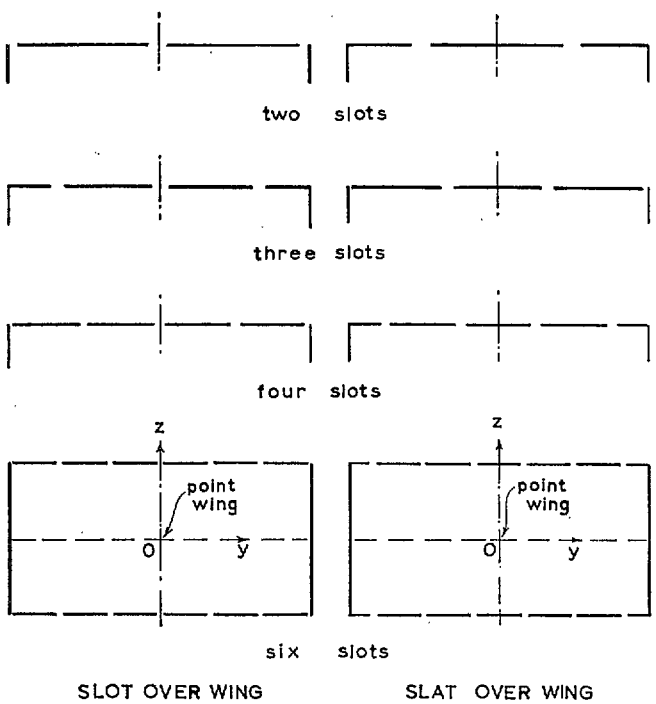

FIG. 1. Position of slots

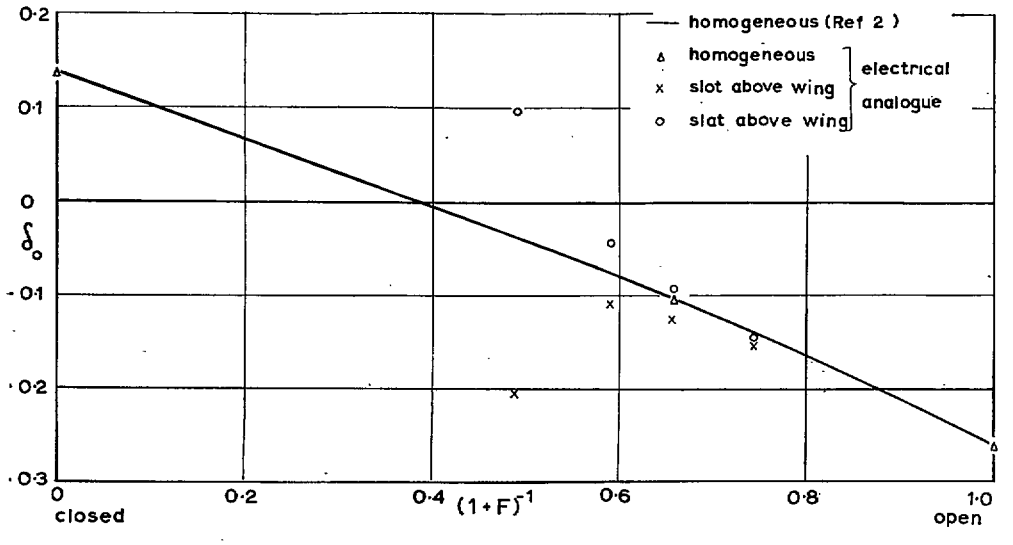

FIG. 2. Comparison of lift interference for duplex tunnel with slotted roof and floor

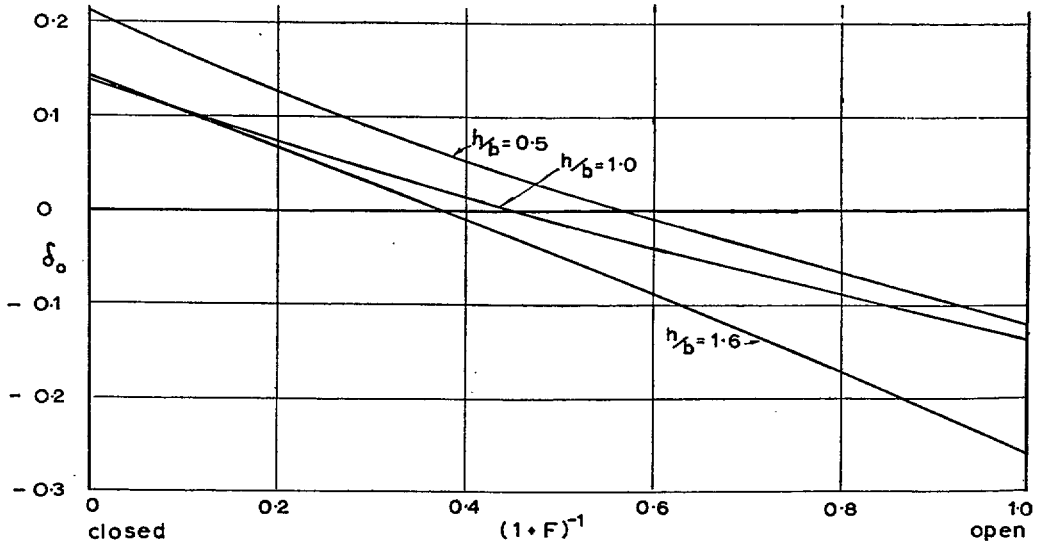

FIG. 3. Lift interference for rectangular tunnels with four walls slotted

Printed in Wales for Her Majesty's Stationery Office by Allens (Cardiff) Limited.

Dd.125874 K5 11/66

Published by
HER MAJESTY'S STATIONERY OFFICE

To be purchased from
49 High Holborn, London W.C.1
423 Oxford Street, London W.1
13A Castle Street, Edinburgh 2
109 St. Mary Street, Cardiff
Brazennose Street, Manchester 2
50 Fairfax Street, Bristol 1
35 Smallbrook, Ringway, Birmingham 5
80 Chichester Street, Belfast 1
or through any bookseller

S.O. Code No. 23-3452